J|A|C|S
ARTICLES
Published on Web 09/13/2007

Borate Binding to Siderophores: Structure and Stability

Wesley R. Harris,*,§ Shady A. Amin,† Frithjof C. Küpper,‡ David H. Green,‡ and Carl J. Carrano*,†

Contribution from the Department of Chemistry and Biochemistry, San Diego State University, San Diego, California 92182-1030, Scottish Association for Marine Science, Dunstaffnage Marine Laboratory, Oban, Argyll PA37 1QA, Scotland, U.K., and Department of Chemistry and Biochemistry, University of Missouri−St. Louis, St. Louis, Missouri 63121

Received May 25, 2007; E-mail: carrano@sciences.sdsu.edu

Abstract: Well-known as specific iron chelating agents produced by bacteria, it is shown that some, but not all, siderophore classes have an unexpected binding affinity for boron. The relevant criterium is the availability of a vicinal dianionic oxygen containing binding group (i.e., citrate or catecholate). The resulting boron complexes have been characterized by ESI-MS, multinuclear NMR, and DFT calculations. Detailed boron binding constants have been measured for vibrioferrin, rhizoferrin, and petrobactin. The observed affinity of certain siderophores for borate, a common chemical species in the marine but not the terrestrial environment, allows for small, but potentially significant, concentrations of B-siderophores to exist at oceanic pH. We hypothesize that these concentrations could be sufficient for them to function as cell signaling molecules or as mediators of biological boron uptake. In addition, binding of the tetrahedral boron to these siderophores results in a conformation that is different from either the free siderophore or its iron complex and would thus allow a distinction to be made between its iron uptake and any putative cell signaling roles.

Introduction

Iron is an essential element for all living organisms due to its ubiquitous role in redox enzymes, especially in the context of respiration and photosynthesis, and marine organisms are no exception to this.[1] However although iron is the fourth most abundant element in the Earth's crust, it is present under aerobic conditions at neutral pH only in the form of extremely insoluble minerals that severely restrict its bioavailability. The iron level in open ocean waters is even lower than those in most terrestrial environments,[2−4] since a large fraction of the limited iron available in the ocean appears to be already tightly complexed.[5,6] Marine bacteria, like their terrestrial counterparts, have evolved sophisticated systems based on high-affinity iron-specific binding compounds called siderophores to acquire, transport, and process this essential, but biologically unavailable, metal ion. Their major role is the extracellular solubilization of iron from minerals and/or organic substrates and its specific transport into microbial cells. Several hundred siderophores, including some from marine environments, are known, and extensive studies of their isolation, structure, transport, and molecular genetics have been undertaken in the past four decades.[7−11] The structural variety of siderophores has been comprehensively reviewed, but they can in general be divided into three groups depending on the ligands used for iron binding.[12] Thus there are hydroxamate, catecholate, and carboxylate type siderophores, as well as those that use some combination of these three functional groups.

Considered essential to their role as iron transporters is the fact that siderophores have both high affinity and high specificity for Fe(III) over other biologically significant cations. We have recently reported the hitherto unrecognized binding of borate to the siderophore vibrioferrin isolated from cultures of a marine bacterium.[14] Here we follow up on that work and show, using a combination of ESI-MS and multinuclear NMR, as well as potentiometric and NMR titrations, that certain well-established siderophores have an unexpectedly high affinity for boron (a cation found in high concentration in seawater)[13] that may be significant for siderophore chemistry under the prevailing chemical conditions in the ocean.

Experimental Section

Siderophore Isolation. Vibrioferrin isolation from *Marinobacter sp.* strain DG870 and DG979 was described previously.[14] A sample of

† San Diego State University.
‡ Dunstaffnage Marine Laboratory.
§ University of Missouri−St. Louis.

(1) Black, K. D.; Shimmield, G. B. *Biogeochemistry of Marine Systems*; Blackwell Publishing: Oxford, U.K., 2003.
(2) Bruland, K. W.; Donat, J. R.; Hutchins, D. A. *Limnol. Oceanogr.* **1991**, *36* (8), 1555−1577.
(3) Martin, J. H.; Fitzwater, S. E. *Nature* **1988**, *331*, 341−343.
(4) Wu, J.; Luther, G. W. *Limnol. Oceanogr.* **1994**, *39* (5), 1119−1129.
(5) Hutchins, D. A.; Witter, A. E.; Butler, A.; Luther, G. W. *Nature* **1999**, *400*, 858−861.
(6) Rue, E. L.; Bruland, K. W. *Limnol. Oceanogr.* **1997**, *42*, 901−910.
(7) Winkelmann, G., Carrano, C. J., Eds. *Transition Metals in Microbial Metabolism*; Harwood Academic Publishers: Amsterdam, The Netherlands, 1997.
(8) Raymond, K. N.; Carrano, C. J. *Acc. Chem. Res.* **1979**, *12*, 183.
(9) Raymond, K. N. *Pure Appl. Chem.* **1994**, *66* (4), 773−781.
(10) Martinez, J. S.; Zhang, G. P.; Holt, P. D.; Jung, H. T.; Carrano, C. J.; Haygood, M. G.; Butler, A. *Science* 2000, *287*, 1245.
(11) Martinez, J. S.; Carter-Franklin, J. N.; Mann, E. L.; Martin, J. D.; Haygood, M. G.; Butler A. *Proc. Natl. Acad. Sci. U.S.A.* **2003**, *100* (7), 3754−3759.
(12) Butler, A. *BioMetals* **2005**, *18*, 369.
(13) Bowen, H. J. M. *Trace Elements in Biochemistry*; Academic Press: London, U.K., 1966.
(14) Amin, S.; Küpper, F. C.; Green, D. H.; Harris, W. R.; Carrano, C. J. *J. Am. Chem. Soc.* **2007**, *129*, 478−479.

petrobactin was kindly provided by Prof. Alison Butler, UCSB, and a sample of rhizoferrin, by Prof. Günther Winkelmann, University of Tübingen.

Potentiometric Titrations. Standard carbonate-free solutions of NaOH were prepared from Dilut-it ampules (Baker) using doubly deionized boiled water and stored under argon, which had been passed over Ascarite. Base solutions were standardized with KHP to the phenolphthalein end point. The absence of carbonate was confirmed by Gran's plot.[15] The potentiometric titrations were performed on a Mettler-Toledo DL50 instrument. The hydrogen ion concentration was measured using a Mettler-Toledo DG111-5C electrode, which was corrected to read the negative log of the hydrogen ion concentration directly using dilute HCl solution. The titrations were performed in a jacketed titration vessel connected to a constant-temperature water bath, which was kept at 25.00 ± 0.05 °C, and the ionic strength was fixed with 0.25 M NaCl. The solution was kept under an argon atmosphere throughout the titration. The ligand protonation constants were determined from nonlinear refinement of the data using the program BEST.[16]

NMR Titrations. All NMR experiments were carried out on a Varian 500 MHz instrument using standard pulse sequences for the ^{1}H and ^{11}B experiments. To eliminate the broad borosilicate background of glass, quartz NMR tubes were used in all titrations. A solution of boric acid at pH 2 was used as a ^{11}B standard throughout the titrations. All boron complexes were obtained by the incremental addition of boric acid from a stock solution, which was prepared by dissolving a known, dried amount of boric acid in D_2O, to a 7 mM solution of siderophore in D_2O. The hydrogen (deuterium) ion concentration was measured using an Accumet AB15 pH meter with an Accumet MicroProbe pH electrode. The electrode was calibrated using standard buffers in H_2O. The meter readings in D_2O were corrected by adding 0.44 to obtain values of pD.[17] The pD titrations were carried out by the addition of NaOD solution, which was prepared by dissolving solid Na in a D_2O solution. The base was standardized by titration against potassium hydrogen phthalate to the phenolphthalein end point. The titration solutions were left to equilibrate for a minimum of 6 h after each addition of NaOD or boric acid.

In the analyses of the NMR titration data, the pK_a values for VF measured in H_2O were corrected to pK_a^D values for use with D_2O solutions. Literature values of pK_a^D were used to prepare a plot of pK_a^D vs pK_a that contained 12 data points representing 8 different acids.[18−20] There is an excellent linear correlation ($r^2 = 0.998$) between pK_a^D and pK_a that is described by the function

$$pK_a^D = (1.031 \pm 0.014)(pK_a) + (0.395 \pm 0.084) \qquad (1)$$

The calculations of effective boron binding constants from NMR data were based on pD and pK_a^D values. The effective binding constants were fitted to various functions of formal binding constants (β^D) and pD. Any values of β^D that involved a deuterium ion as an explicit reactant or product were then corrected to β values for H_2O by use of eq 1. Since eq 1 is based on pK_a's for monoprotic reactions (i.e., stepwise pK_a values, rather than overall β values), the equilibrium constants measured for boron binding to siderophore were formulated as single-proton, stepwise constants and then corrected to the appropriate value for H_2O solutions. Effective binding constants, for which the overall proton stoichiometry was not known, have not been corrected and are reported as K^D_{eff} values that are valid for D_2O solutions.

Electrospray-Ionization Mass Spectrometry. High-resolution mass spectra were obtained on a Micromass (Manchester, U.K.) QTOF-2 time-of-flight mass spectrometer (made available to us at UCSB by the courtesy of Prof. Alison Butler) with an electrospray ionization source. Samples (in aqueous solution, 30 mM NH_4HCO_3 buffer or methanol) were injected by a Harvard Apparatus (Holliston, Massachusetts 01746, USA) infusion pump at a rate of 5 μL/min. For exact mass measurements an internal standard of known mass (H9985, an octapeptide with $m/z = 829.5393$), was co-infused with the samples of free vibrioferrin (VF) or the borate−vibrioferrin complex (BVF). The exact mass measured for the parent peak of BVF in negative ion mode of 440.0971 agrees to within 4.1 ppm with that calculated for $C_{16}H_{18}{}^{10}BN_2O_{12}$ (440.0989). Routine ESI-MS and MS^n spectra were obtained on a Finnigan LCQ ion-trap mass spectrometer equipped with an ESI source (Finnigan MAT, San Jose, CA). MS/MS spectra were obtained utilizing a collision voltage between 20 and 50 V and argon as the collision gas. Isotope distribution patterns were simulated using the program IsoPro 3.0

Results

Boron Binding to Vibrioferrin. In the process of searching for new siderophores from *Marinobacter* sp. DG870 and 979, species of marine bacteria associated with the toxic dinoflagellate *G. catenatum*, we isolated by HPLC from XAD extracts of spent culture medium a species that we identified as the boron complex of the known carboxylate siderophore vibrioferrin (VF).[14] Since boron was not a component of the artificial seawater media used in culturing DG 870 and 979, the boron incorporated into VF could only have been derived from the borosilicate glass flasks, suggesting a strong sequestering ability of VF for B. The structure of vibrioferrin is shown in Figure 1.

Based on ^{13}C NMR shifts, we have shown in a preliminary communication that the reaction of vibrioferrin with borate involves the two α-hydroxycarboxylate functional groups of the ligand.[14] Each of these groups interacts in a bidentate fashion, binding to boron via one carboxylate oxygen and a deprotonated α-hydroxy group. By utilizing both functional groups, vibrioferrin displaces the OH^- groups from boric acid and forms a stable tetrahedral complex with boron(III).

Addition of increments of boric acid to a solution of VF at around pD 2.6 revealed changes in the ^{1}H and ^{11}B NMR spectra indicative of a mixture of free borate and the boron−VF complex in slow exchange on the NMR time scale. Since water is an expected product of the reaction between borate and VF (*vide infra*), it is not surprising that the degree of borate binding is highly solvent dependent. Thus while a mixture of millimolar borate and VF in water shows peaks in the ^{11}B NMR experiment corresponding to free and bound borate of approximately equal intensity, the free borate peak is much smaller in acetonitrile and unobservable in DMSO (Figure 2).

Figure 3 shows a plot of complex formed in D_2O vs equivalents of boric acid added that indicates the formation of a 1:1 B−VF complex. The curvature of the plot suggests a modest overall stability constant. Formal metal−ligand stability constants are defined as

$$\beta_{ijk} = \frac{[M_iL_jH_k]}{[M]^i[L]^j[H^+]^k} \qquad (2)$$

Formal binding constants are typically expressed using the fully deprotonated form of the free ligand. Ligand deprotonation constants have been measured by potentiometric titration with standardized NaOH. The only groups that are deprotonated over the pH range of 2−12 are the three carboxylic acid groups. The

(15) Gran, G. *Analyst* **1952**, *77*, 661−670.
(16) Martell, A. E.; Motekaitis, R. J. *The Determination and Use of Stability Constants*; Wiley-VCH Inc.: New York, 1992.
(17) Krezel, A.; Bal, W. *J. Inorg. Biochem.* **2004**, *98*, 161−166.
(18) Covington, A. K.; Paabo, M.; Robinson, R. A.; Bates, R. G. *Anal. Chem.* **1968**, *40*, 700−706.
(19) Gary, R.; Bates, R. G.; Robinson, R. A. *J. Phys. Chem.* **1964**, *68*, 3806−3809.
(20) Glasoe, P. K.; Long, F. A. *J. Phys. Chem.* **1960**, *64*, 188−190.

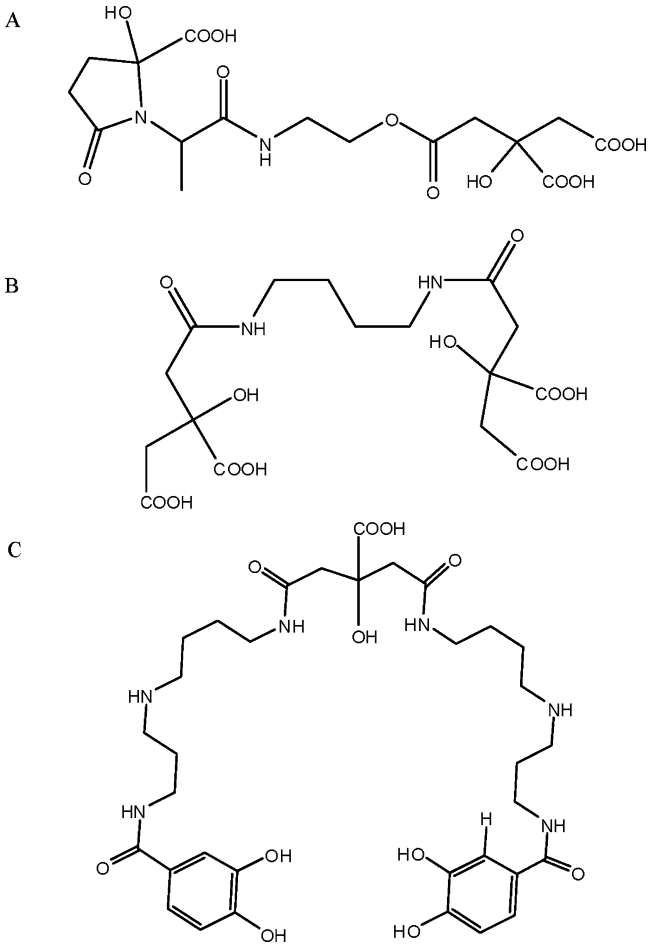

Figure 1. Structure of the siderophores used in this study: (A) vibrioferrin in its predominant closed chain form, (B) rhizoferrin, (C) petrobactin.

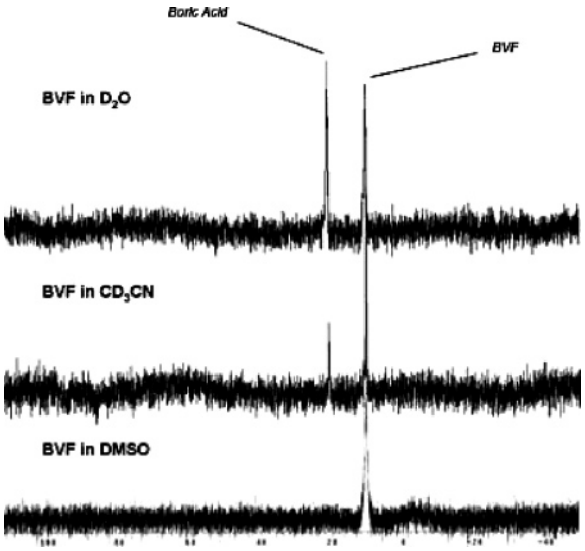

Figure 2. ^{11}B spectra of a mixture of boric acid and vibrioferrin in D_2O, acetonitrile, and DMSO. The peak near 20 ppm corresponds to free boric acid, while the peak at 8.5 ppm represents a boron−vibrioferrin complex.

analysis of the potentiometric data gave successive pK_a values of 5.13, 3.60, and 2.71.

In this study, boric acid is treated as the free metal ion, and the equilibrium expression for boron binding to VF is thus

$$H^+ + B(OH)_3 + VF^{3-} \rightleftarrows B(H_{-2}VF)^{2-} + 3\,H_2O \quad (3)$$

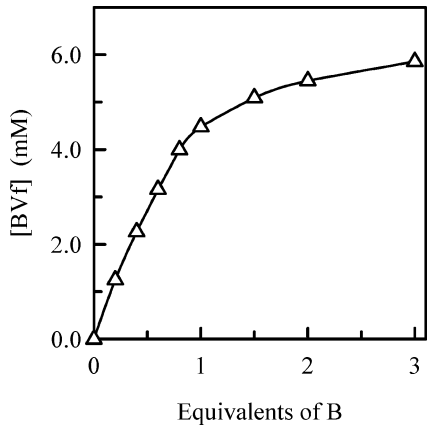

Figure 3. Titration of 6.4 mM vibrioferrin with boric acid at pD 2.6, showing the concentration of the borate−vibrioferrin complex as a function of added boric acid.

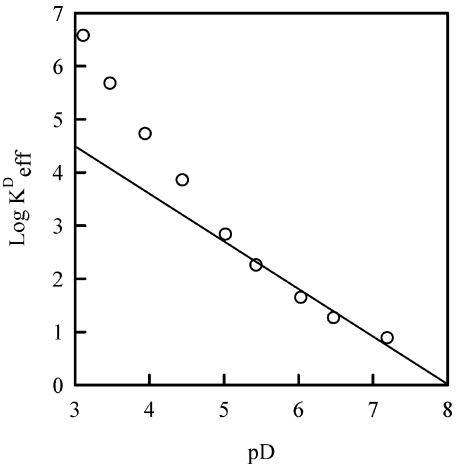

Figure 4. Plot of log K^D_{eff} for the formation of borate−vibrioferrin complexes vs the solution pD.

The formation of the tetrahedral boron−VF complex involves the displacement of the three −OH groups from the boric acid as three water molecules. This requires the addition of three protons. Two of these protons are generated internally by the deprotonation of the α-hydroxyl groups of vibrioferrin; thus the complexed form of vibrioferrin is shown as H_{-2}VF. The third proton comes from the solution and is shown as a reactant in eq 3. Based on the formalism defined in eq 2, the equilibrium shown in eq 3 corresponds to the binding constant

$$\beta_{111} = \frac{[B(H_{-2}VF)^{2-}]}{[B(OH)_3][VF^{3-}][H^+]} \quad (4)$$

This expression can be rearranged to define an effective binding constant that is valid at a specific pH as in eq 5,

$$K_{eff} = \beta_{111}[H^+] = \frac{[B(H_{-2}VF)^{2-}]}{[B(OH)_3][VF^{3-}]} \quad (5)$$

Values of K^D_{eff} have been obtained from NMR data at a series of pD values. Based on eq 5 we expected that a plot of log K_{eff} vs pD would be linear with a slope equal to −1 and an intercept equal to the log of the overall binding constant β_{111}. A plot of log K^D_{eff} vs pD is shown in Figure 4. Clearly the plot is not

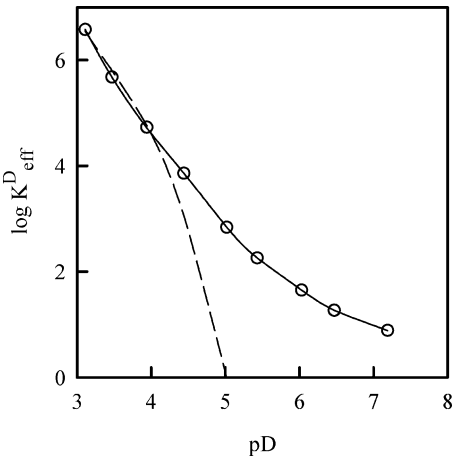

Figure 5. Plot of log K^{D}_{eff} vs pD for the binding of borate by vibrioferrin. The solid line shows the calculated plot from a least-squares fit of the data to eq 8, while the dashed line shows the calculated plot from a least-squares fit of the data to eq 7.

linear over the entire pD range. The segment of the plot from pD 5.0 to 7.2 is linear with the expected slope of $n = -0.9 \pm 0.10$. However, it is clear that log K^{D}_{eff} has a steeper pD-dependence as the pD decreases below 5. We interpret these data as indicating that the $B(H_{-2}VF)^{2-}$ complex undergoes an additional protonation at the lower pD values. Thus the equilibrium model was expanded to include the species $B(H_{-1}VF)^{1-}$. Formation of such a species would require two protons as reactants in order to release three water molecules from $B(OH)_3$ and would be described by the formation constant β_{112} based on the formalism defined in eq 2. The ^{11}B NMR experiments only show signals for bound and free boron and do not distinguish between $B(H_{-2}VF)^{2-}$ and $B(H_{-1}VF)^{-}$. Therefore an analysis of the NMR data directly yields an effective binding constant defined as

$$K^{D}_{eff} = \frac{([B(H_{-2}VF)^{2-}] + [B(H_{-1}VF)^{-}])}{[B(OH)_3][VF^{3-}]} \qquad (6)$$

This K^{D}_{eff} is related to formal binding constants by the equation

$$K^{D}_{eff} = \beta^{D}_{111}[D^{+}] + \beta^{D}_{112}[D^{+}]^2 \qquad (7)$$

We attempted to calculate values for β^{D}_{111} and β^{D}_{112} from a least-squares fit of K_{eff} vs [D] using eq 7 and the commercial software package TableCurve.[21] The calculation included a $1/y$ weighting factor to prevent the fit from being completely dominated by the larger K^{D}_{eff} values. There was a reasonably good fit to the data, but the calculation resulted in a physically meaningless negative value for β^{D}_{111}. The equilibrium model was then expanded to include a third species, such that K^{D}_{eff} was defined as

$$K^{D}_{eff} = \beta^{D}_{111}[D^{+}] + \beta^{D}_{112}[D^{+}]^2 + \beta^{D}_{113}[D^{+}]^3 \qquad (8)$$

Values of K^{D}_{eff} vs $[D^{+}]$ were then fitted to eq 8. The use of eq 8 gave an improvement in the least-squares fit that was highly significant as judged from the F_{stat} parameter calculated by TableCurve. To illustrate the improvement in the fit, Figure 5 shows the original data from Figure 4 along with the calculated lines associated with eqs 7 and 8. The plot clearly shows that the data conform to eq 8. Thus, three β^{D}_{ijk} values were calculated from the fit to eq 8 and corrected to H_2O solution using eq 2. These corrected values for β_{ijk} are listed in Table 1.

Table 1. Formal Binding Constants, β_{ijk}, for Boron Complexes with Vibrioferrin and Petrobactin

	i	*j*	*k*	log β_{ijk}	complex pK_a
$B(H_{-2}VF)^{2-}$	1	1	1	7.34 ± 0.10	--
$B(H_{-1}VF)^{1-}$	1	1	2	11.21 ± 0.04	3.87
B(VF)	1	1	3	14.10 ± 0.02	2.89
$B(H_{-3}PB)^{-}$	1	1	0	5.04 ± 0.07	--
$B(H_{-2}PB)$	1	1	1	11.54 ± 0.16	6.5

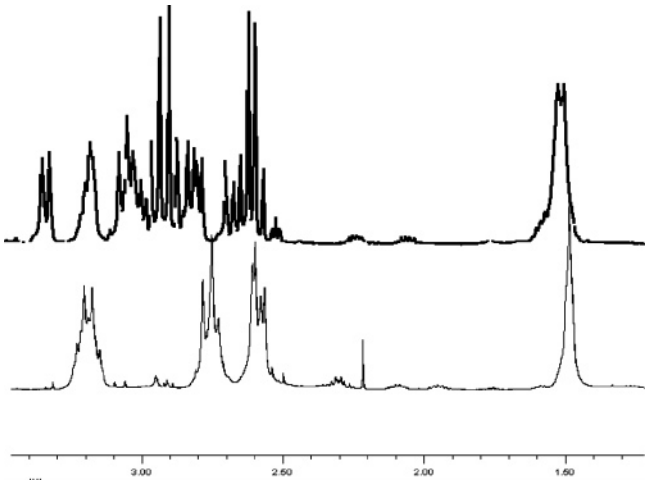

Figure 6. ^{1}H NMR spectra for rhizoferrin in the presence (upper) and absence (lower) of 1 equiv of boric acid at pD 2.48.

The borate titration data shown in Figure 3 were collected at pD 2.60. The predominant boron containing species at this pD would be the B−VF complex described by the binding constant β_{113}. An effective binding constant for pD 2.60 based on eq 8 would be log $K^{D}_{eff} = 8.0$. The effective binding constant calculated from the data in Figure 3 is log $K^{D}_{eff} = 8.25 \pm 0.09$.

Boron Binding to Rhizoferrin. Although we have not analyzed it in the same detail as in the case for VF, we note that the related dicitrate siderophore rhizoferrin, RF (Figure 1), also binds borate as determined by HPLC, ESI-MS, and ^{11}B, ^{1}H, and ^{13}C NMR (see Supporting Information). The ^{1}H NMR spectrum of free RF and RF in the presence of borate at pD 2.48 is shown in Figure 6. The ^{13}C spectrum indicates that the RF molecule retains its twofold symmetry when bound to boron as only eight resonances are observed. Again the only significant coordination-induced shifts were for carbons 3 (13) and 6 (16) indicating binding of the boron through the two citrate moieties. The ^{11}B peak at 9.5 ppm is close to that observed for VF providing further evidence that the binding mode is similar for both. ESI-MS of a solution of B−RF shows a peak cluster at 443 amu with the appropriate isotope pattern indicative of a 1:1 borate complex. To evaluate the possible structure of such a 1:1 borate−RF complex we used the 10 lowest energy conformers of the complex obtained from MMFF conformational searching algorithms as implemented in Spartan '02[22] followed by geometry optimization at the DFT level (B3LYP) using Jaguar (Schroedinger). The resulting lowest energy structure is shown in Figure 7. The overall structure is very

(21) *TableCurve 2D*; SYSTAT Software, Inc.; Richmond, CA, 2002.

(22) *Spartan '02*; Wavefunction Inc.: Irvine, CA, 2002.

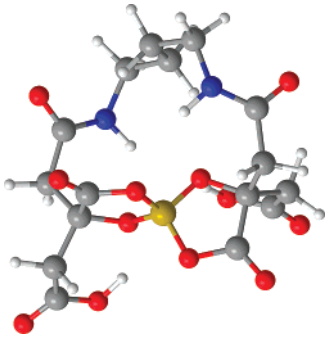

Figure 7. Geometry optimized structure (DFT) of the lowest energy conformer of boron−rhizoferrin.

similar to that proposed for the $B(H_{-1}VF)^{1-}$ complex and is stabilized by a number of internal hydrogen bonds. The effective boron affinity of RF, log $K^{D}_{eff} = 10.6$ at pD 2.48, as determined by ^{11}B NMR titration, is significantly larger than the effective binding constant of VF of log $K^{D}_{eff} = 8.32$ as calculated for this pD from eq 8.

Boron Binding to Petrobactin. Having established that simple dicitrate-type siderophores such as VF and RF both have a significant affinity for boron, the question arises whether this is an unrecognized property of all classes of siderophores. To examine this issue we looked at petrobactin, a siderophore with mixed carboxylate/catecholate functionality. The structure of petrobactin (PB) is shown in Figure 1. Since PB contains both citrate and catecholate groups, either of which, in principle, could bind to boron, we conducted ^{1}H NMR titrations that clearly reveal that the binding of petrobactin to boron is not through the citrate group as in vibrioferrin but rather through the two catecholate functionalities (Figure 8). The sharp ^{1}H NMR peaks revealed for B−PB are suggestive of a well-defined structure. The ^{11}B NMR spectrum reveals a peak at 8.8 ppm, very close to that found for the spiro-diester formed by VF.[23] Using the structural data gleaned from the ^{1}H and ^{11}B NMR, we again determined the 10 lowest energy conformers of the complex using MMFF conformational searching algorithms. Several of the lowest energy conformers were then geometry optimized at the DFT level (B3LYP), the lowest energy structure of which is shown in Figure 9.

Quantitative boron binding experiments were conducted next. There are seven potentially dissociable protons in the ligand, two phenolic protons from each of the two catechol groups, two protonated secondary amines, and the central carboxylic acid. However, the reported potentiometric titration of petrobactin detects the dissociation of only three groups, with successive pK_a values of 9.77, 7.95, and 3.13.[24] The pK_a value of 3.13 can be assigned to the single carboxylate group. It is more difficult to assign the two higher pK_a values to specific functional groups, since the intrinsic pK_a values of secondary amines and catechol groups overlap. However, it is not necessary to assign the macroscopic pK_a values to specific functional groups in order to measure the boron−PB binding constants.

Since we can only measure pK_a values for the loss of three protons from fully protonated H_7PB^{2+}, it is necessary to redefine the "fully deprotonated" form of the ligand as the monoanion. As noted above, the precise location of the remaining four dissociable protons on the ligand is not known, but for convenience we will assume that the amines are deprotonated and that all four of the catechol oxygens are protonated.

Effective binding constants for the boron−PB complex have been determined from both ^{1}H and ^{11}B NMR data collected over the pD range of 6.8 to 9.4. The calculations of K^{D}_{eff} incorporated both the ligand pK_a^{D} values and a pK_a^{D} of 9.63 for boric acid. Based on the interactions of borate with catechol and the NMR titrations, we had expected that petrobactin would coordinate boron through all four of the phenolic groups in the ligand. The equilibrium for this reaction would then be

$$B(OH)_3 + PB^{1-} \overset{\beta_{11-1}}{\rightleftharpoons} B(H_{-4}PB)^{2-} + H^+ \qquad (9)$$

where the three water molecules produced in the forward reaction have been omitted for clarity.

The description of the bound ligand as $H_{-4}PB^{5-}$ reflects the loss of four protons in addition to the three protons for which we have measured pK_a values. If eq 9 accurately described the binding reaction, we would define the effective binding constant as $K_{eff} = \beta_{11-1}/[H^+]$, and we would expect that a plot of log K^{D}_{eff} vs pD would have a slope of 1. Instead, the plot of K^{D}_{eff} vs pD between pD 6 and 9 shown in Figure 10 has a slope of -0.2 ± 0.04. Such a small slope indicates that borate binding in this system consists primarily of the reaction

$$B(OH)_3 + PB^{1-} \overset{\beta_{110}}{\rightleftharpoons} B(H_{-3}PB)^{1-} \qquad (10)$$

where the three water molecules produced in the forward reaction here and in the subsequent equation have again been omitted for clarity.

If one ignores the pD dependence and simply calculates a simple mean value for the binding constant, the result is that log $K^{D}_{eff} = 5.1 \pm 0.2$ for eq 10.

Although the pH dependence of the B−PB binding is small, it is still statistically significant. To account for the negative slope of the plot in Figure 10, it is necessary to include the equilibrium

$$B(OH)_3 + PB^{1-} + H^+ \overset{\beta_{111}}{\rightleftharpoons} B(H_{-2}PB) \qquad (11)$$

Based on eqs 10 and 11, the pH dependence of K_{eff} would be

$$K_{eff} = \beta_{110} + \beta_{111}[H^+] \qquad (12)$$

A fit of K^{D}_{eff} vs $[D^+]$ to eq 12 was used to determine β^{D}_{110} and β^{D}_{111}. The expression for β_{110} contains no protons; therefore the equilibrium for H_2O is the same as that for D_2O, i.e., $\beta_{110} = \beta^{D}_{110}$. The p$K_a^{D}$ for the protonated complex was corrected using eq 1. The corrected values for β_{110} and β_{111} are listed in Table 1.

The final equilibrium model for PB is summarized in Figure 11. Given the inherently high pK_a's of the catechol groups in petrobactin, it is not necessarily surprising that protons are retained in the boron complex. In Figure 11 these protons have been arbitrarily placed on the secondary amines. A speciation diagram for the B−PB system for the conditions of the NMR titrations is shown in Figure 12. Because of the higher basicity of the ligand functional groups, there is virtually no boron

(23) (a) Pizer, R.; Ricatto, P. J. *Inorg. Chem.* **1994**, *33*, 2402−2406. (b) Semmelhack, M. F.; Campagna, S. R.; Hwa, C.; Federle, M. J.; Bassler, B. L. *Org. Lett.* **2004**, *6*, 2635−37.
(24) Amin, S.; Butler, A.; Küpper, F. C.; Carrano, C. J. Unpublished results.

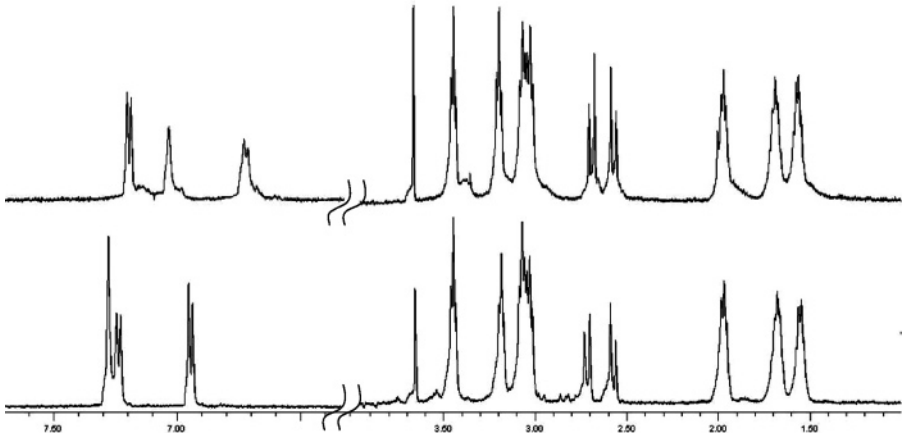

Figure 8. ^{1}H NMR spectra of petrobactin in the presence (upper) and absence (lower) of 1 equiv of boric acid at pD 8.49.

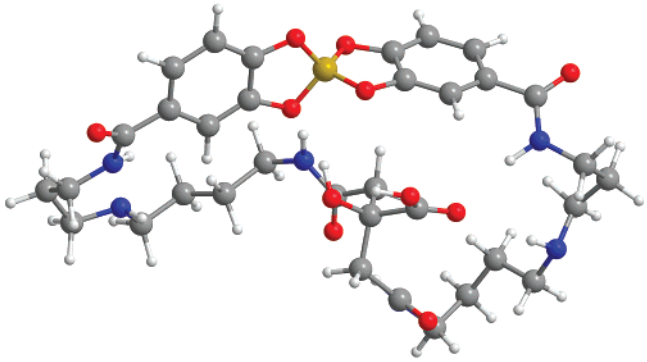

Figure 9. Geometry optimized structure (DFT) of the lowest energy conformer of boron−petrobactin.

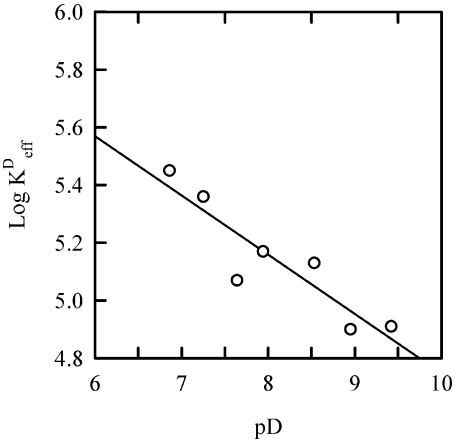

Figure 10. Plot of log K^{D}_{eff} vs pD for the binding of borate to petrobactin.

binding at low pH, where the ligand is highly protonated. However, as the pH increases to approximately 7, the higher binding affinity of the catecholate groups results in the conversion of a large percentage of the petrobactin into the B(H$_{-3}$PB)$^{1-}$ complex. In order to produce a significant binding of borate to PB, the pH must be above the pK_a of 6.5 for the B(H$_{-2}$PB) complex. As a result, the B(H$_{-2}$PB) complex accumulates to a maximum of only about 3%. Because of the low degree of formation of this complex, there is less confidence in the value reported for log β_{111}.

Boron Binding to Aerobactin. Given the boron affinity that we have observed for the dicarboxylate siderophores VF and RF, and the catecholate petrobactin, we also examined the boron binding affinity of the other major siderophore class that has been found in marine microbes, the hydroxamates. The hydroxamates constitute the longest-known and largest group of siderophores. We have therefore examined the ability of the dihydroxamate siderophore aerobactin, which has been isolated both from terrestrial sources and from several marine *Vibrio* species, to bind boron. Using a combination of HPLC, ESI-MS, and NMR, we could find no evidence for boron binding by aerobactin at any pH between 2 and 9. No boron binding was evident even in more nonpolar solvents such as DMSO, where the binding of boron to VF was shown to be essentially complete and irreversible. Indeed no boron binding was detected for any of the hydroxamate siderophores we tested (data not shown).

Discussion

α-Hydroxy Acid Binding. The α-hydroxy acid moiety has long been known to bind significantly to borate. Indeed the structure of a variety of salts of "borodicitrate" have been reported where the boron is bound in a tetrahedral fashion through the carboxylate and deprotonated α-hydroxyl groups from each of two citrates.[25] Such a binding mode was also confirmed for VF whose ^{13}C coordination-induced shifts and position of the peak in the ^{11}B NMR at 8.5 ppm are completely consistent with a spiro-borate diester structurally analogous to borodicitrate. Mass spectrometry and ^{11}B and ^{1}H NMR also suggest a similar mode of binding for another dicitrate siderophore, rhizoferrin.

The pH-dependence of boron binding by VF represents a complex balancing of factors. Increasing the pH decreases the effective binding constants, since the formal binding constants include protons as reactants. Conversely, increasing the pH up to approximately pH 6 increases the fraction of the unbound ligand in the deprotonated form, which increases the effective binding constant. In the pH range from 2 to 5, these factors largely offset one another and the percentage of boric acid bound to VF is relatively constant. However, once all the ligand has been converted to the deprotonated VF^{3-} form, further increases in pH results in a sharp decrease in the effective binding constant. This behavior is illustrated by the speciation diagram shown in Figure 13.

(25) Zviedre, I.; Fundamenskii, V. S.; Krasnikov, V. V.; Kolesnikova, G. P. *Zh. Strukt. Khim.* **1984**, *25* (4), 95−101.

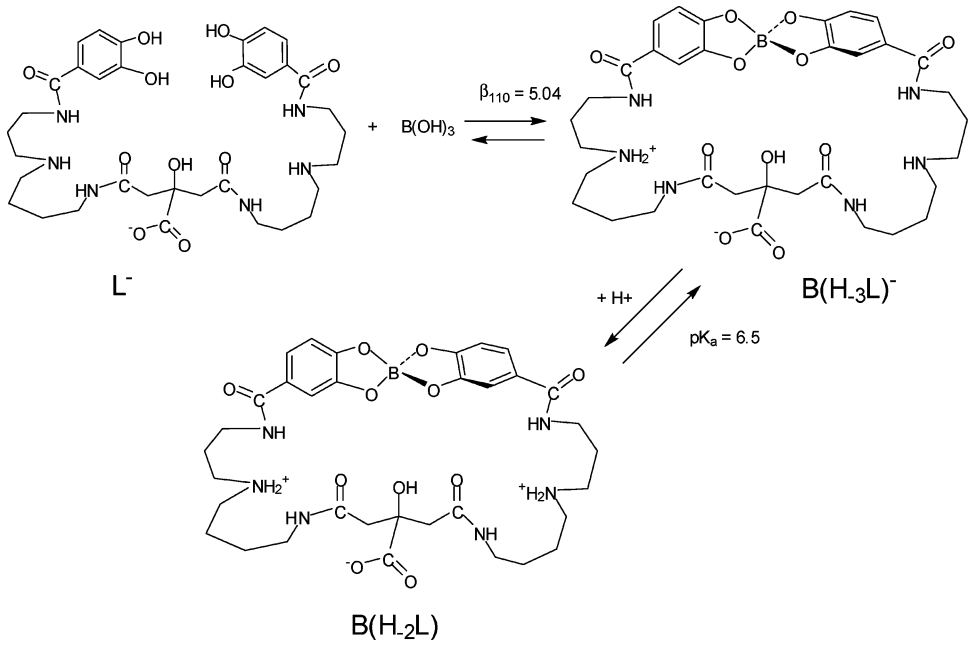

Figure 11. Proposed equilibrium model for the borate−PB system.

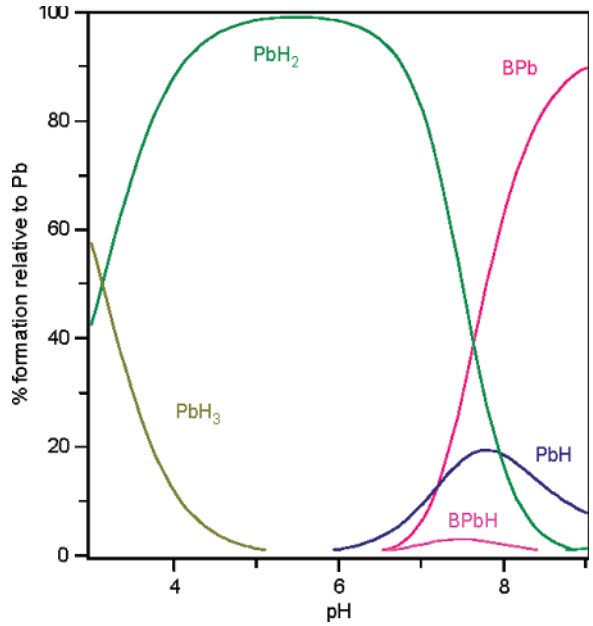

Figure 12. Speciation diagram for a mixture of 3.5 mM petrobactin and 3.9 mM borate as a function of pH.

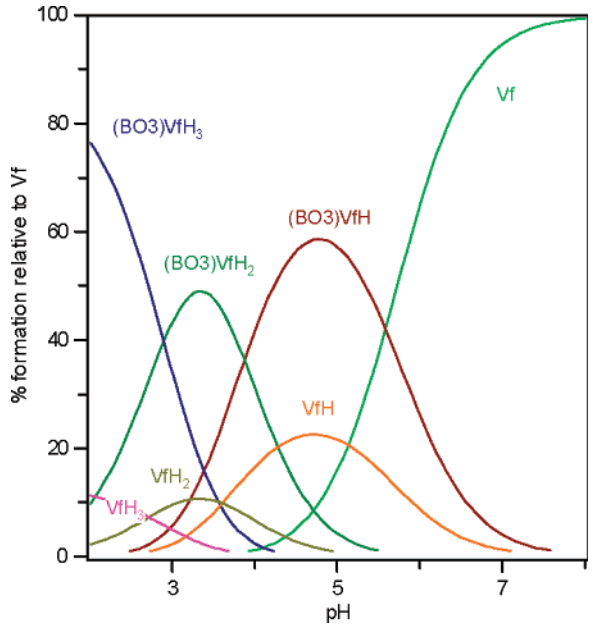

Figure 13. Speciation diagram for a mixture of 6.0 mM vibrioferrin and 20 mM boric acid as a function of pH.

Catechol Binding. Martell and Smith list two binding constants for the reaction of catechol with boric acid.[26] The 1:1 and 2:1 complexes are described, respectively, by the constants

$$\beta_{11-1} = \frac{[\mathrm{L} - \mathrm{B(OH)_2}][\mathrm{H^+}]}{[\mathrm{B(OH)_3}][\mathrm{H_2L}]} = 10^{-5.13} \qquad (13)$$

$$\beta_{12-1} = \frac{[\mathrm{B(L)_2}][\mathrm{H^+}]}{[\mathrm{B(OH)_3}][\mathrm{H_2L}]^2} = 10^{-4.84} \qquad (14)$$

The value for β_{12-1} for catechol corresponds to an effective binding constant $\beta^*_2 = 10^{3.16}$ at pH 8. The effective binding constant for PB at this pH is $10^{5.04}$. Thus there appears to be a significant chelate effect associated with the binding to PB. Since the catecholate groups in PB are so widely separated in the ligand structure, the magnitude of the chelate effect suggests that the complex is stabilized by internal hydrogen bonding interactions.

Hydroxamate "Binding". Siderophores have been divided into three major groups depending on the donor atoms utilized in iron binding, i.e., the catecholate, hydroxamate, and carboxylate classes. Mixed siderophores are also well-known. We have shown here that boron binding is significant for some, but not all, of these siderophore classes. The notable exceptions are the hydroxamates, which, although the largest class of siderophores, do not show boron binding at any pH. Previous reports in the literature indicate that simple hydroximates but

(26) Martell, A. E.; Smith, R. M. *Critical Stability Constants*; Plenum Press, New York, U.S.A., 1974.

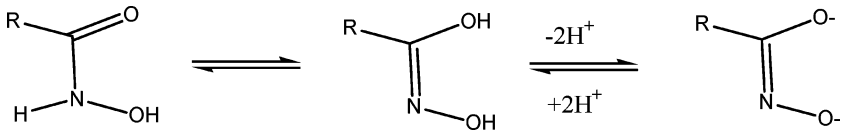

Figure 14. Resonance forms of hydroximates.

not hydroxamates are capable of binding boron.[27] This has been bourn out by our work. The relevant criterion appears to be a vicinal dianionic dioxygen binding group (i.e., citrate or catecholate). Hydroximates have a resonance structure (Figure 14) that allows this while the N-substituted hydroxamates that make up all known siderophores of this class do not.

Biological Implications. Given the binding constants and other properties we have described here, what might be the biological implications (if any) of the ability of some siderophores to bind boron? Curiously, the first borate−siderophore complex, B−vibrioferrin, was isolated from the culture media of a bacterial "symbiont" of a toxic marine dinoflagellate, suggesting that it may have a biological function for the algal partner of the symbiosis. Despite the fact that boron is an essential trace element for various species of phytoplankton,[28,29] these calculations suggest it is less likely that VF has a direct role in boron uptake to either the producing bacteria or the dinoflagellate partner at pH 8.0 typical of seawater. However, boron binding to VF is strongly enhanced at lower pH and in solvents other than water as shown by the fact that boron binding to VF is essentially complete and irreversible in DMSO as compared to H_2O. Thus in either an acidic or less polar microenvironment, such as in a membrane or vesicle, boron binding by VF could be greatly enhanced. Membrane associated boron transporters have recently been described in both plants and animals although an extracellular boron scavenger is unknown.[30,31]

The calculated binding of boron to PB under marine environmental conditions is much more significant than is the case for VF. Nevertheless, bacteria are not known to have an absolute dietary requirement for boron suggesting that its primary purpose is not to bind and transport boron. If a direct uptake and transport role for boron is less likely, the question remains as to what its biological significance may be.

While siderophores are known to have as their primary function the binding and transport of iron from the environment into microbial cells, increasing evidence suggests that they may also play another significant role as signaling molecules. "Quorum sensing" is the term used to describe the cell density-dependent regulation of bacterial physiology, including gene expression.[32,33] Quorum sensing bacteria excrete low molecular weight chemical "messenger" molecules into the environment, which when a critical concentration is reached, trigger a signal transduction cascade. This signal cascade results in an alteration of gene expression, ostensibly in a population-dependent manner. Siderophore production and other iron transport genes are among those long reported to be under "quorum sensing" control.[34,35] An additional link between quorum sensing and iron regulation has been uncovered with the observation that certain quorum sensing molecules also possess the ability to bind iron and thus influence siderophore production and use.[36,37] Of more direct relevance are the numerous recent reports that siderophores themselves can have a cell signaling function in addition to their iron uptake and transport roles. For example pyoverdin is reported to regulate not only its own production but also that of several other secreted virulence factor proteins in *P. aeruginosa*.[38] Siderophores produced by one species of marine bacteria have also been reported to induce production of siderophores from a previously nonproducing and unrelated bacterium.[39,40]

Simplistically, a quorum sensing role for siderophores might provide a convenient rationale for what has long been an enigma in the area of marine siderophores—namely, why should free living marine bacteria produce and excrete a metabolically expensive molecule such as a siderophore if there is such a low probability of its recapture and uptake into the cell, as would be the case in an open aqueous environment? What however if there were a reasonable chance for recapture and uptake, such as would be present when there were a large number of bacteria in a small space such as a biofilm or other microniche? From this point of view it would be reasonable for siderophores to be produced in large amounts when conditions for successful recapture exist, i.e., under a type of quorum sensing control. Indeed an alternative view of the whole quorum sensing concept is that it is actually a diffusion sensing, rather than a direct population sensing, phenomenon.[41] If we accept for the moment the concept of siderophores as quorum sensing molecules, what then is the relationship to boron binding?

Structurally characterized boron-containing natural products are confined to just a few macrolide antibiotics and a bacterial quorum-sensing molecule known as AI-2.[42,43] We believe that it is highly significant that virtually all of these molecules originate from marine organisms. Most telling is that AI-2 functions as a signal molecule in its boronylated form in marine environments but in its unboronylated form in terrestrial ones.[44] The observed affinity of certain siderophores for borate, a common chemical species in the marine but not the terrestrial environment, allows for significant concentrations of B-sidero-

(27) Fields, A. R.; Daye, B. M.; Christian, R. *Talanta* **1966**, *13*, 929−937.
(28) Lewin, J.; Chen, C. *J. Exp. Bot.* **1976**, *27*, 916−921.
(29) McLauchlan, J. *Phycologia*, **1977**, 16:329−338.
(30) Takano, J.; Noguchi, K.; Yasumori, M.; Kobayashi, M.; Gajdos, Z.; Miwa, K.; Hayashi, H.; Yoneyama, T.; Fujiwara, T. *Nature* **2002**, *420*, 337−340.
(31) Park, M.; Li, Q.; Shcheynikov, N.; Zeng, W.; Muallem, S. *Mol. Cell* **2004**, *16*, 331−341.
(32) Federle, M. J.; Bassler, B. L. *J. Clin. Invest.* **2003**, *112*, 1291−1299.
(33) See articles in Quorum Sensing/Metabonomics, Metabolomics and Metabolic Profiling, special issue, *Anal. Bioanal. Chem.* **2007**, 387.
(34) Guan, L. L.; Kamino, K. *BMC Microbiol.* **2001**, *1*, 1−27.
(35) Fong, K. P.; Gao, L.; Dumuth, D. R. *Infect. Immun.* **2003**, *71*, 298−308.
(36) Kaufmann, G.; Sartorio, R.; Lee, S.; Rogers, C. J.; Meijler, M. M.; Moss, J. A.; Clapham, B.; Brogan, A. P.; Derson, T. J.; Janda, K. D. *Proc. Natl. Acad. Sci. U.S.A.* **2005**, *102*, 309−314.
(37) Diggle, S. P.; Matthjis, S.; Wright, V. J.; Fletcher, M. P.; Chhabra, S. R.; Lamont, I. L.; Kong, X.; Hider, R. C.; Cornelis, P.; Camara, M.; Williams, P. *Chem. Biol.* **2007**, *14*, 87−96.
(38) Lamont, I. L.; Beare, P. A.; Ochsner, U.; Vasil, A. I.; Vasil, M. L. *Proc. Natl. Acad. Sci. U.S.A.* **2002**, *99*, 7072−7077.
(39) Guan, L. L.; Onuki, H.; Kamino, K. *Appl. Environ. Microbiol.* **2000**, *66*, 2797−2803.
(40) Guan, L. L.; Kanoh, K.; Kamino, K. *Appl. Environ. Microbiol.* **2001**, *67*, 1710−1717.
(41) Redfield, R. J. *Trends Microbiol.* **2002**, *10*, 365−369.
(42) Chen, T. S. S.; Chang, C.; Floss, H. G. *J. Am. Chem. Soc.* **1979**, *101*, 5826.
(43) Chen, X.; Schauder, S.; Potier, N.; Van Dorsselaer, A.; Pelczer, I.; Bassler, B. L.; Hughson, F. M. *Nature* **2002**, *415*, 545−549.
(44) Miller, S. T.; Xavier, K. B.; Campagna, S. R.; Taga, M. E.; Semmelhack, M. F.; Bassler, B. L.; Hughson, F. M. *Mol. Cell* **2004**, *15*, 677−687.

phores to exist even at oceanic pH. These concentrations, although small, could well be sufficient for them to function as signaling molecules. Binding of the tetrahedral boron to these siderophores will also result in a conformation that would be different from either the free siderophore or its iron complex, allowing a distinction to be made between its iron uptake and any cell signaling roles. Experimental work designed to address these issues is underway.

Acknowledgment. This publication was prepared under NOAA grant NA04OAR4170038, California SeaGrant College Program project R/CZ-198, through NOAA's National SeaGrant College Program, U.S. Dept. of Commerce. The authors thank Günther Winkelmann, University of Tübingen for a sample of rhizoferrin and Alison Butler, University of California, Santa Barbara for a sample of petrobactin.

Supporting Information Available: Structure of Rf and numbering scheme; additional ^{13}C, ^{1}H, ^{11}B NMR and ESI-MS data for rhizoferrin and boronylated rhizoferrin. This material is available free of charge via the Internet at http://pubs.acs.org.

JA073788V